Acicular Ferrite Morphologies in a Medium-Carbon Microalloyed Steel

I. MADARIAGA, I. GUTIERREZ, and H.K.D.H. BHADESHIA

The influence of time and isothermal transformation temperature on the morphology of acicular ferrite in a medium-carbon microalloyed steel has been studied using optical and transmission electron microscopy (TEM). This study has been carried out with the analysis of the microstructures obtained with one- and two-stage isothermal treatments at 400 °C and 450 °C, following austenitization at 1250 °C. The heat treatments were interrupted at different times to observe the evolution of the microstructure at each temperature. The results show that a decrease in the isothermal transformation temperature gives rise to the development of sheaves of parallel ferrite plates, similar to bainitic sheaves, but intragranularly nucleated. These replace the face-to-edge nucleation that dominates the transformation at higher temperatures. The TEM observations reveal that the plates correspond to upper acicular ferrite and the sheaves to lower acicular ferrite. In this last case, cementite precipitates are present at the ferrite unit interiors and between the different platelets.

I. INTRODUCTION

ACICULAR ferrite and bainite are considered to be formed by the same transformation mechanism.[1–4] Both microstructures develop in the same range of temperatures: below the high temperatures where allotriomorphic ferrite or pearlite form, but above the martensite-start temperature. In bainite, the ferrite initiates at the austenite grain boundaries, forming sheaves of parallel plates with the same crystallographic orientation, whereas acicular ferrite is nucleated intragranularly at nonmetallic inclusions.[5,6] The process of nucleation on the inclusions, together with the autocatalytic nucleation,[7] leads to a chaotic arrangement of plates and the fine-grained interlocking microstructure characteristic of acicular ferrite.[7,8]

Most of the work on acicular ferrite has been carried out on welds.[9–12] The high density of inclusions present in steel weld deposits ensures a high density of nucleation sites, which favors the development of an acicular ferrite microstructure instead of a bainitic one. Several authors have focused on the study of acicular ferrite nucleation at inclusions,[13–16] and a variety of mechanisms have been proposed to explain the nucleation event, as reported elsewhere.[1,2,8] Some inclusions have been identified to favor the nucleation of the acicular ferrite and have been used to inoculate steel and produce this type of microstructure in the base material and not only in the weld pool.[17–23]

Acicular ferrite has also been developed in a medium-carbon forging steel[24–28] or a low-carbon steel[29] following a conventional processing route. The lower density of inclusions, as compared to that of weldments, would be expected to cause an increase of the volume fraction of bainite, at the expense of acicular ferrite. However, in the steel used in this study, this difficulty is avoided thanks to the nature, crystallography, and spatial configuration of the nucleating inclusions, as has been previously reported.[26,27,28] As in the case of the acicular ferrite developed in low-carbon steels,[29,30] the fine-grained microstructure obtained in these medium-carbon steels also ensures a good combination of mechanical properties.[24,25,31–33]

In the present article, the influence of the time and temperature of the isothermal treatment on the morphology of the acicular ferrite formed in a medium-carbon steel has been investigated. The investigation has been focused on the development of the microstructure once the nucleation event has taken place. The work includes the study of the different transformation products obtained during the isothermal transformation of the austenite. The fine details of the various microstructures produced have been resolved using transmission electron microscopy (TEM) and scanning electron microscopy.

II. EXPERIMENTAL PROCEDURE

The chemical composition of the commercial steel used in the present work is presented in Table I. Isothermal treatments were conducted in cubic samples with 10-mm-long sides, which were austenitized at 1250 °C in an inert argon atmosphere, followed by direct quenching in a salt bath at 400 °C and 450 °C for different times (between 10 seconds and 20 minutes) before a final water quenching.

To analyze the transformation in the bulk, avoiding surface effects such as oxidation and decarburization, samples were sectioned into two pieces, which were mechanically polished and etched in 2 pct nital for optical metallography.

Thin-foil preparation for TEM observation was carried out on the samples treated for 10 seconds at 450 °C and for 20 seconds at 400 °C. The thin foils were prepared after slicing rods of 3 mm in diameter into discs which were thinned to 80 to 100 μm by mechanical polishing and electropolished using 5 pct perchloric acid, 25 pct glycerol, and 70 pct ethanol solution. The polishing potential was 20 V at a current of 80 mA. The study of the thin foils was carried

I. MADARIAGA, Researcher, is with ITP, Parque Tecnologico de Zamudio, 48170 Vizcaya, Spain. I. GUTIERREZ, Principal Researcher, Materials Department, and Head, Thermomechanical Treatments Group, is with CEIT and the University of Navarra (ESI), 20018 San Sebastian, Basque Country, Spain. H.K.D.H. BHADESHIA, Professor, is with the Department of Materials Science and Metallurgy, University of Cambridge, Cambridge CB2 3QZ, United Kingdom.

Manuscript submitted October 20, 2000.

Table I. Chemical Composition of Microalloyed Steel (Weight Percent)

C	Mn	Si	P	S	Cr	Mo	V	Cu	Al	Ti	N
0.37	1.45	0.56	0.01	0.043	0.04	0.025	0.11	0.14	0.024	0.015	0.0162

out in a PHILIPS* CM12 electron microscope operating at

*PHILIPS is a trademark of Philips Electronic Instruments Corp., Mahwah, NJ.

100 kV and equipped with an EDAX 9190 energy-dispersive spectrometer (EDS).

The amount of retained austenite at room temperature was measured by X-ray diffraction, using standard techniques,[34,35] with a PHILIPS IPW1825/00 diffractometer controlled by an APD1700 data treatment system and using a computer program, according to the method proposed by Maeder *et al.*[36] The errors in retained-austenite measurements were estimated to be <10 pct of the absolute value, in all cases.

III. RESULTS

The microstructures obtained after 20 minutes of isothermal treatment at 450 °C and 400 °C can be seen in the micrographs of Figures 1(a) and (b), respectively. In both cases, the austenite has transformed to acicular ferrite, giving rise to the characteristic interlocking microstructure. However, in spite of the clearly acicular morphology, there are slight differences between the two samples. These differences are better appreciated when the earlier stages of the transformation are studied.

The microstructures developed after 10 and 20 seconds at 450 °C are shown in Figures 2(a) and (b), respectively, while the results obtained with the treatments carried out for 10 and 30 seconds at 400 °C are presented in Figures 2(c) and (d), respectively. Comparing the micrographs corresponding to 10 seconds of isothermal treatment at 450 °C and 400 °C, it can be seen that at the initial stages, the transformation proceeds identically in both cases. The nucleation of the first acicular ferrite units takes place intragranularly at nonmetallic inclusions present in the austenite. The transformation kinetics are faster at 450 °C than at 400 °C. The main differences at the early stages are that there is a decrease in the number density of plates and a reduction of their aspect ratio, for the lowest treatment temperature.

Differences in the microstructure obtained at the two temperatures become pronounced as the transformation progressed beyond 10 seconds, *i.e.*, after the initiation of the first generation of plates from inclusion nucleation sites. Figures 2(c) and (d) show that whereas at 400 °C the second generation of plates developed in a parallel sheaf formation, transformation at 450 °C progressed with the stimulation of nonparallel plates. This is evident also from the transmission electron micrographs presented in Figure 3. However, as can be seen in Figure 4, even if the differences in morphology of the acicular ferrite become more apparent as the transformation progresses, they are also present from the early stages.

The volume fraction of retained austenite, measured in the samples after quenching to room temperature from the previously mentioned isothermal transformation temperatures, can be seen in Figure 5. It is clear from the shape of the curves that the isothermal transformation at 450 °C and 400 °C involves two steps. For short holdings, the amount of retained austenite increases with time, reaching a maximum, after which the volume fraction of austenite undergoes a rapid decrease toward zero. The time to reach the peak and the magnitude of it depend on the transformation temperature. For 450 °C, a maximum volume fraction of retained austenite (10 pct) is observed after 1 minute of isothermal holding, whereas for 400 °C, the peak is at 20 seconds and the volume fraction for this treatment is 5 pct.

For the treatments carried out at 400 °C, carbides have been observed by TEM to form after relatively short treatment times, as can be seen in Figures 6 and 7. The interpretation of the diffraction patterns has revealed that these

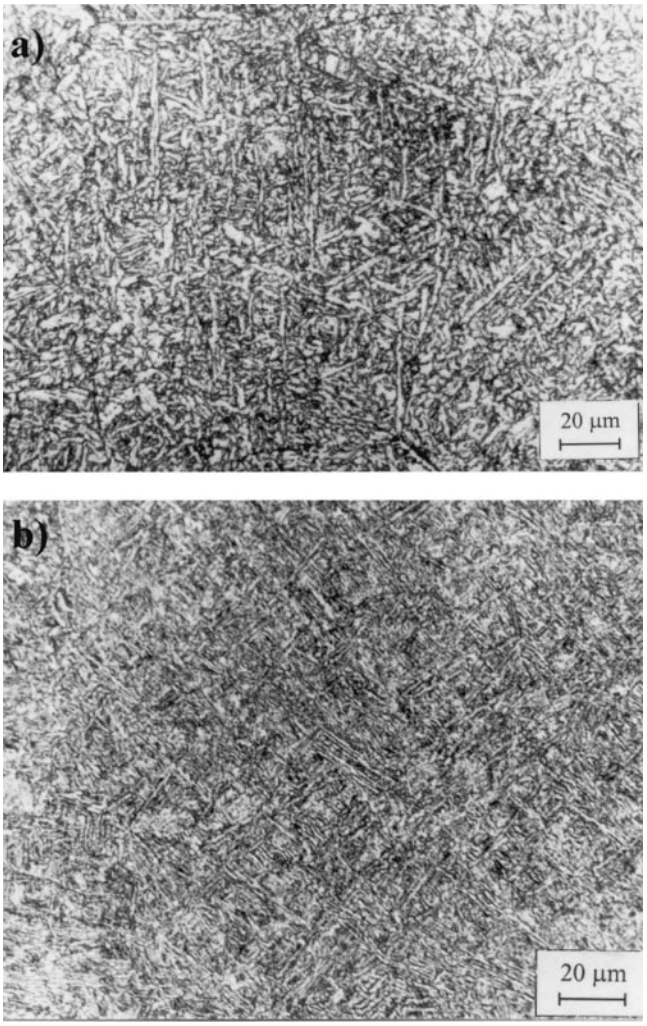

Fig. 1—Microstructures obtained after 20 min of isothermal treatment: (*a*) 450 °C and (*b*) 400 °C.

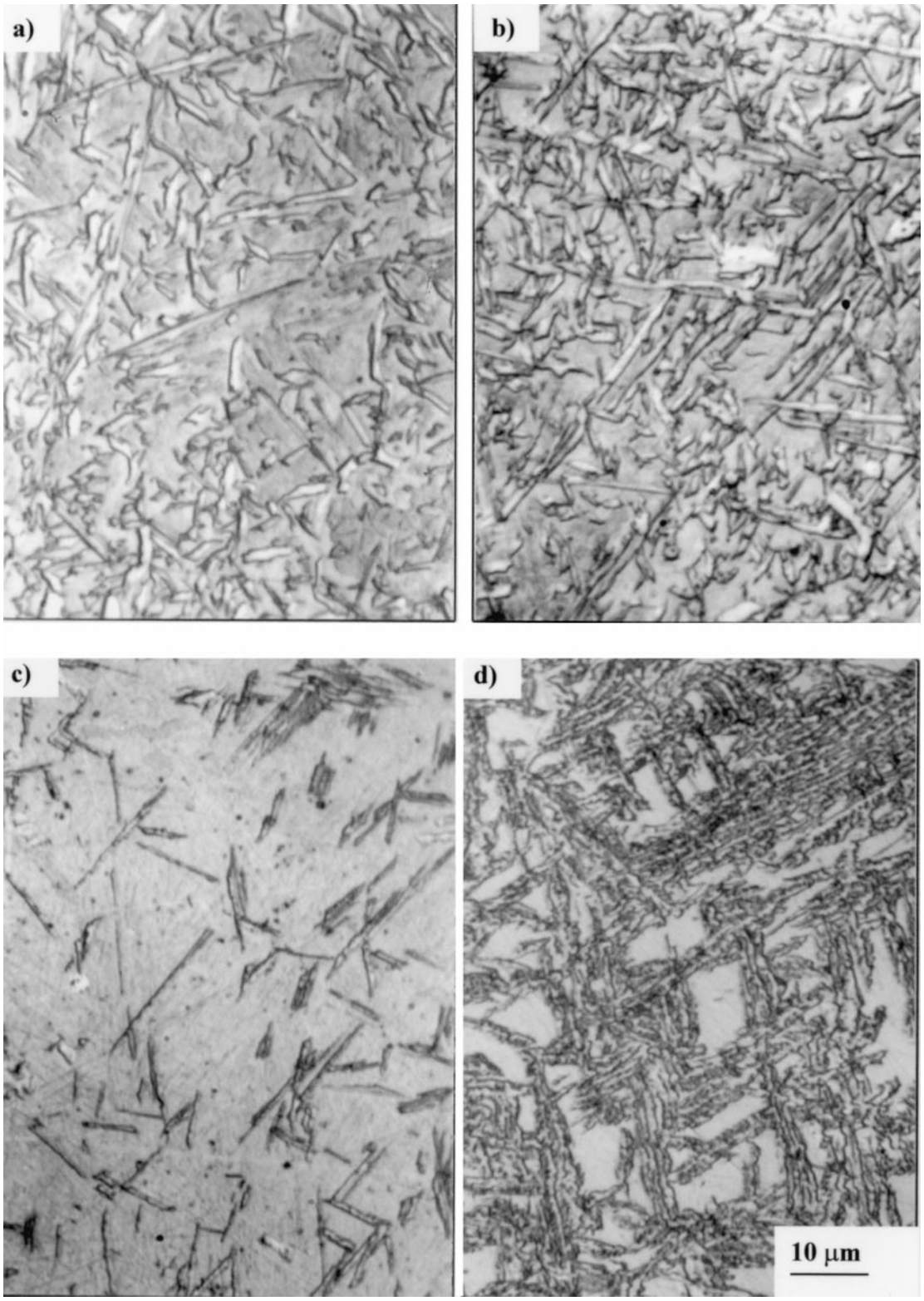

Fig. 2—Time evolution of the microstructures obtained with isothermal treatments: (*a*) 10 s at 450 °C, (*b*) 20 s at 450 °C, (*c*) 10 s at 400 °C, and (*d*) 30 s at 400 °C.

carbides are cementite. This same observation technique was used to investigate the orientations of different ferrite units belonging to a given sheaf. As can be seen in Figure 8, the different parallel units have the same crystallographic orientation. For the isothermal treatments carried out at 450 °C, in general, no carbides were observed to form within the ferrite plates. They only were produced in the interplate regions for treatment times beyond 1 minute.

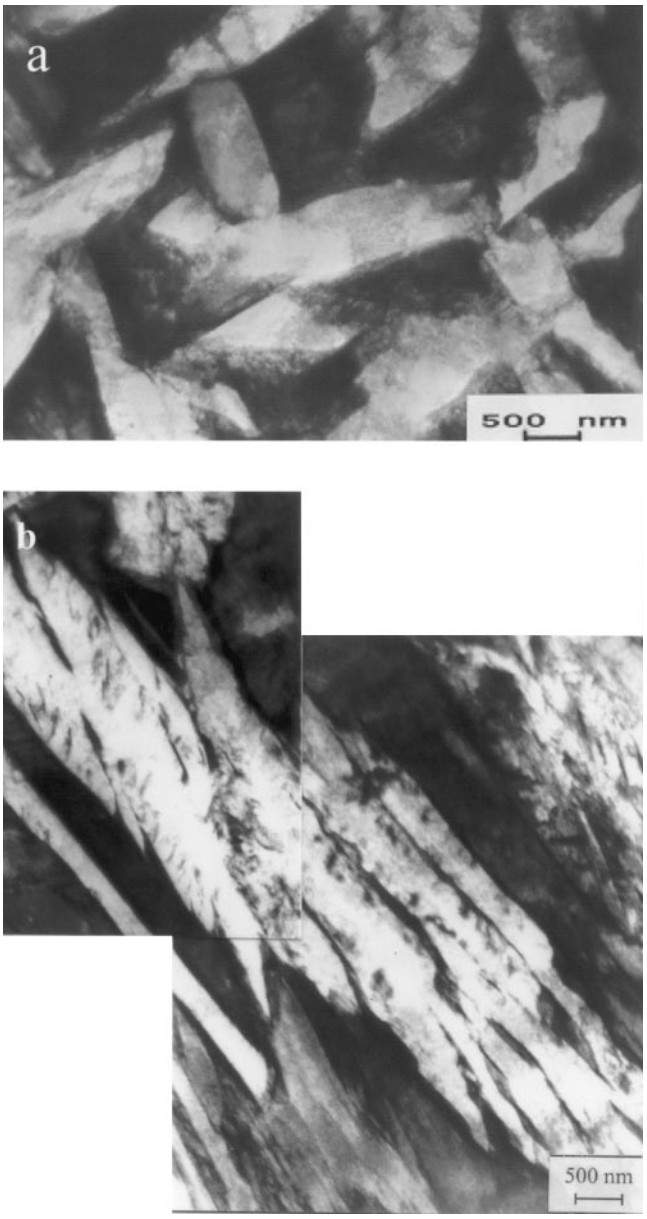

Fig. 3—TEM image of the beginning of the transformation at 450 °C and 400 °C: (*a*) 10 s at 450 °C and (*b*) 20 s at 400 °C.

IV. DISCUSSION

All the isothermal heat treatments carried out on the present steel, after austenitization, led to the intragranular nucleation of acicular ferrite. The first ferrite plates have been observed to nucleate on sulfide particles formed by a MnS core and a shell of CuS. This seems to play an important role in favoring the nucleation of acicular ferrite, as discussed elsewhere.[27,28]

However, two different microstructural morphologies are produced, depending on the isothermal treatment temperature. At high temperatures, the secondary plates nucleated at the interface between the primary ones and austenite are inclined at a high angle with respect to the substrate unit. This produces the typical acicular ferrite interlocked microstructure, as shown in Figure 3(a). At lower treatment temperatures, a significant change in the morphology of the acicular ferrite is clearly apparent, and the final microstructure could be incorrectly identified as being bainitic, without the pictures for the early stages of transformation. It is observed that the nucleation of the primary plates takes place intragranularly on the same second-phase particles, as reported before, and not at grain boundaries, as would be the case for bainite. In the treatments carried out at 400 °C, a clear tendency to form sheaves is observed, and the final microstructure is composed of packets of plates following the same growth direction, as is shown in Figure 3(b).

The growth of both bainite and acicular ferrite causes an invariant plane-strain shape deformation, which gives rise to a stress field in the adjacent austenite.[37] The field is such that an identical variant is stimulated in the vicinity of the tip of the original plate, whereas an accommodating variant is favored on the face of the original plate.

There is a unique relationship between the shape deformation, orientation relationship, and habit plane. This means that it is not possible (in the absence of degenerancies) to have two plates with an identical habit plane but different shape deformation. It follows that plates nucleated on the face of a substrate plate must have a different habit plane and orientation, leading to a chaotic microstructure. By contrast, a plate nucleating at the tip of the substrate plate must be an identical variant with the same habit plane and orientation, giving rise to a sheaf microstructure.

It remains to be discovered why, in the context of autocatalytic nucleation, face nucleation is favored at 450 °C while tip nucleation occurs at 400 °C.

It has been reported that a sheaf morphology is not usually observed in acicular ferrite microstructures, due to the effect of hard impingement taking place between plates nucleated independently at adjacent sites.[38] The microstructural observations carried out in the present work reveal that from the early stages of the transformation, significant differences in the morphology of the acicular ferrite can be distinguished, as is clearly illustrated by the micrographs in Figure 4. At 450 °C, single plates form at second-phase particles, while at 400 °C, different parallel platelets are formed with residual phases between them. Impingement does not seem to play an important role, at this stage, in the formation of either type of morphology.

Additionally, in Figure 9(a), different individual plates formed after 10 seconds of treatment at 450 °C can be observed. Growth of these plates is not limited by impingement, and it is clearly apparent that the tendency to form subunits is very reduced. Only very few incipient irregularities, such as the ones indicated by the arrows on the micrograph, broke the regularity of the plate/austenite interfaces. This clearly indicates that impingement is not the mechanism responsible for the transition between both types of microstructures.

It is to be mentioned, however, that longer treatment times at 450 °C, leading to the formation of greater acicular ferrite volume fractions, tend to increase the irregularity of the ferrite/austenite interface, as can be seen in Figure 9(b). This seems to indicate that, after the formation of the plates at 450 °C, some additional growth of the plates still remains possible, which produces these irregularities in the ferrite/austenite interface.

The growth of the acicular ferrite plates probably takes place, as in the case of bainite, without carbon diffusion.

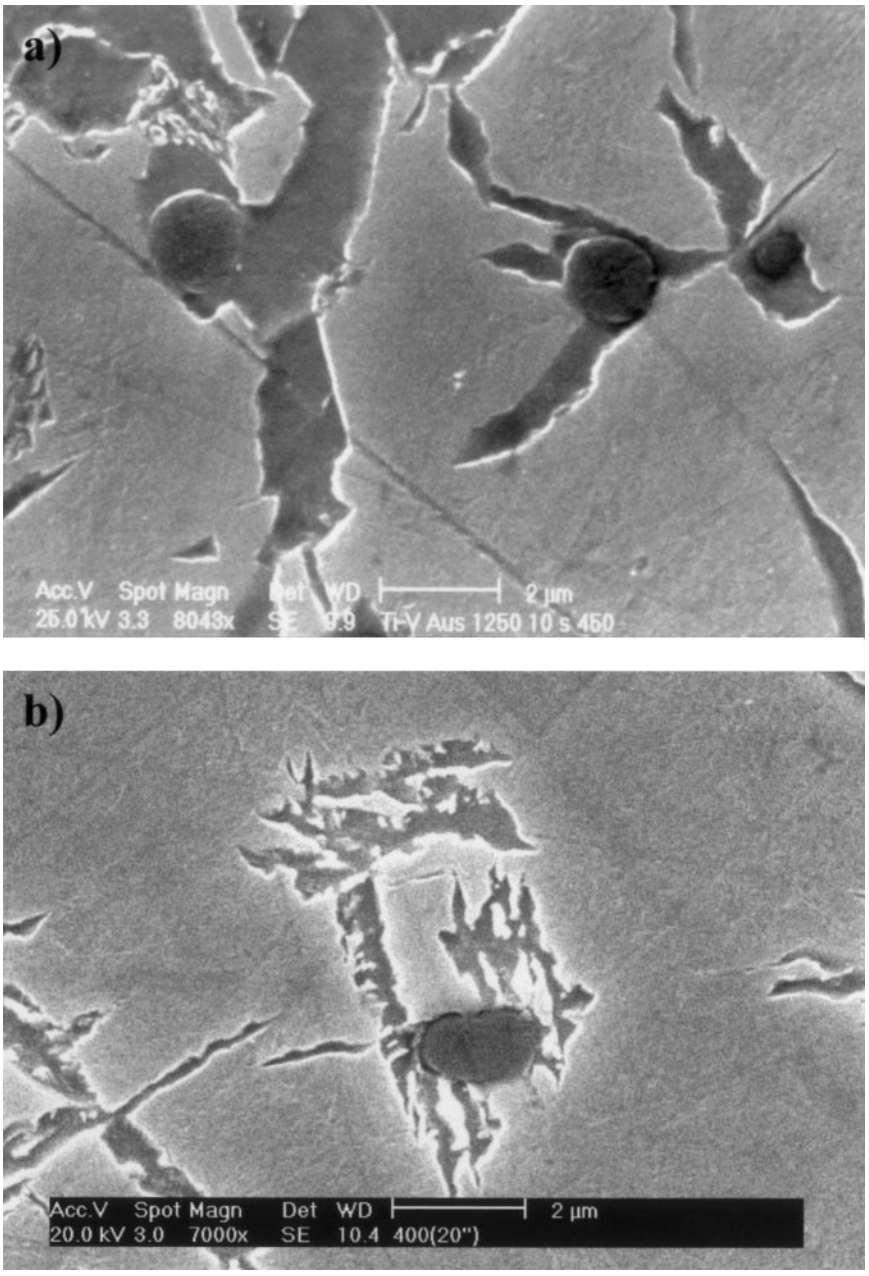

Fig. 4—Acicular ferrite units nucleated at second-phase particles: (*a*) sheaf morphology produced at 400 °C and (*b*) plate morphology produced at 450 °C.

The excess carbon in ferrite is probably rejected into the austenite soon after. Part of the carbon-enriched austenite (~10 pct) remains stable on quenching to room temperature, as can be seen in Figure 5. For longer treatment times, the transformation of this austenite to ferrite plus carbides causes a decrease of the volume fraction of this phase that is present at room temperature.[39,40] It is to be noted that the appearance of the perturbations on the ferrite/austenite interface, observed when passing from 10 to 20 seconds of treatment at 450 °C, occurs within the range of austenite carbon enrichment, in agreement with the results in Figure 5. These perturbations probably indicate that the growth of each individual plate proceeds, after nucleation, by the fast growth of a supersaturated ferrite plate. Soon after, the ferrite plate decarburizes, but, given that impingement is low at this stage, the plate can to some extent continue growing as before, but now probably in a locally carbon-enriched austenite. The perturbations could be due to differences in the carbon distribution in front of the interface, as the diffusion field in austenite is expected to be heterogeneous.

In spite of these perturbations, the morphology of the acicular ferrite is significantly different from that developed at 400 °C, for the same interval of treatment times, as can be seen in Figure 10.

Autocatalytic formation of plates not associated directly with particles contributes significantly to the progress of the transformation. It is clear that at 450 °C the secondary plates, nucleated on the face of the substrate plate, grow as individual plates. At 400 °C, there is a tendency to form sheaves both for the primary units nucleated on particles and the secondary ones formed autocatalytically. At 400 °C, autocatalysis also produces nucleation of secondary units at a high

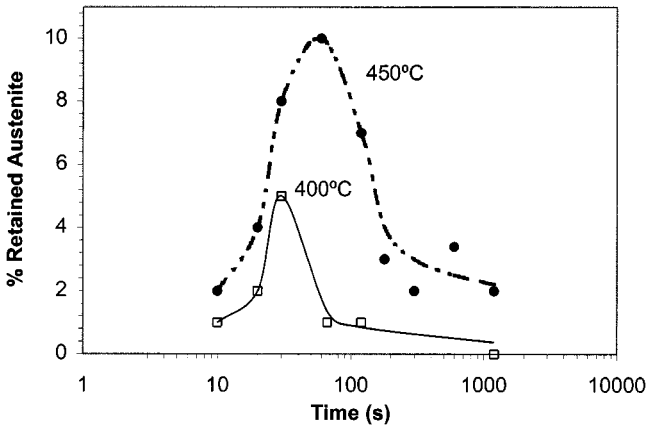

Fig. 5—Retained austenite content as a function of the isothermal treatment time and temperature.

angle to the primary ones, as can be seen in Figure 11. However, even in this case, the progress of the transformation leads to the formation of ferrite sheaves growing now from the primary sheaf/austenite interface.

The TEM work has revealed that, in most cases, the ferrite units belonging to the same sheaf have the same crystallographic orientation (Figure 8). The apparent units are connected, forming one unique ferrite crystal without a grain or subgrain boundary between them. This could indicate that branching of the original ferrite plate has probably been responsible for the sheaf formation and that this, at least in the present case, is more a question of growth than one of nucleation of different self-accommodating units slightly misoriented. One additional and fundamental point observed by TEM is the presence of carbides associated with the ferrite plates. These can clearly be observed in Figure 6. The carbides, identified by diffraction patterns as cementite, are elongated, and most of them form an angle of about 50 deg to the ferrite/austenite interface. The configuration exhibited is the typical one described previously for lower bainite.[41] Diffraction patterns have been used to investigate the crystallographic orientation between cementite and ferrite. The diffraction pattern in Figure 6 shows two sets of spots, one of them belonging to ferrite and the other one to cementite. The interpretation of these patterns allows one to deduce a clear orientation relationship between both phases of the type proposed by Bagaryatskii,[42] as can be seen in the corresponding stereographic projection in the same figure. This clearly indicates that the precipitation of the cementite has taken place from the ferrite, as in the case of lower bainite.[41] However, not all the diffraction patterns agree with the same type of orientation relationship. The pattern in Figure 7 shows again two sets of spots, one corresponding to ferrite and the other one to cementite. The Bagaryatskii orientation relationship would require the parallelism between the $(100)_{cem}$ plane of the cementite and one of the $\{011\}_\alpha$ family of the ferrite. However, as can be seen in the figure, the angle existing between the planes $(100)_{cem}$ and $\{\bar{1}10\}_\alpha$ is 74 deg, which is not compatible with any variant of the orientation relationship between ferrite and cementite proposed by Bagaryatskii. On the contrary, cementite can be assumed to form from austenite following an orientation relationship with the parent phase of the type established by Pitsch.[43] If, at the same time, the austenite is related to the ferrite with the following variant of the Kurdjumov–Sachs[44] orientation relationship:

$$(1\bar{1}0)_\alpha \parallel (11\bar{1})_\gamma \qquad [111]_\alpha \parallel [011]_\gamma$$

the orientation relationships between ferrite and cementite (*via* austenite) can be easily deduced with matrix calculations,[45] leading to the following expressions:

$$73.5 \text{ deg between } (100)_{cem} \text{ and } (\bar{1}10)_\alpha$$

$$17.4 \text{ deg between } (0\bar{1}1)_{cem} \text{ and } (\bar{1}10)_\alpha$$

which agree with the orientations found in the diffraction pattern. This result suggests that carbide precipitation from the carbon-enriched austenite between the ferrite platelets also takes place during the isothermal treatment at 400 °C.

The presence of carbide within the ferrite subunits and between them indicates that the obtained microstructures at 400 °C, in the present steel, correspond to lower acicular ferrite. On reducing the transformation temperature, like in the case of bainite formation, the time required for the decarburization of the ferrite becomes higher than that for the precipitation of cementite, which takes place from supersaturated ferrite. However, the presence of retained austenite at room temperature, for a range of treatment times, as shown in Figure 5, indicates that some carbon enrichment of this phase also takes place during transformation, in agreement with what has been reported for lower bainite.[40,41] This carbon is mainly concentrated between the ferrite subunits until it precipitates, leading to the formation of cementite from austenite. This explains the orientation relationship based on the Pitsch relation found between some cementite particles and ferrite. The precipitation of cementite from supersaturated austenite explains the observed decrease of the volume fraction of γ retained at room temperature, as the treatment time increases.

At 450 °C, the partitioning of carbon from ferrite to austenite is high enough to produce a carbide-free acicular ferrite of the upper type. The results in Figure 5 agree with the mentioned partitioning being higher at 450 °C than at 400 °C.

According to the present results, the development of sheaves is associated with the lower acicular ferrite, while the formation of plates at higher transformation temperatures relates to upper acicular ferrite formation.

The microstructure produced by the isothermal treatments in this steel is mainly acicular ferrite, as pointed out before. However, it still possible to find, in certain localized places, bainite formed on grain boundaries, as shown in Figure 12. It can be seen, in Figure 12(a), that the bainite formed at 450 °C is composed of a set of different ferrite plates growing from the grain boundaries and presenting regular interfaces with the parent austenite. As the treatment time increases, at this same temperature, these interfaces become less regular (Figure 12(b)). This behavior is similar to that exhibited by the acicular ferrite formed at this same temperature. At 400 °C, the different subunits constituting the lower bainite have more irregular interfaces. Carbides are present at the interiors, and some branching leading to different platelets is observed. According to this, it can be said that the different morphologies observed in acicular ferrite relate to those present in the bainite formed for the same steel and treatment conditions. The main difference may arise from the nucleation sites. In the case of bainite, repeated nucleation takes

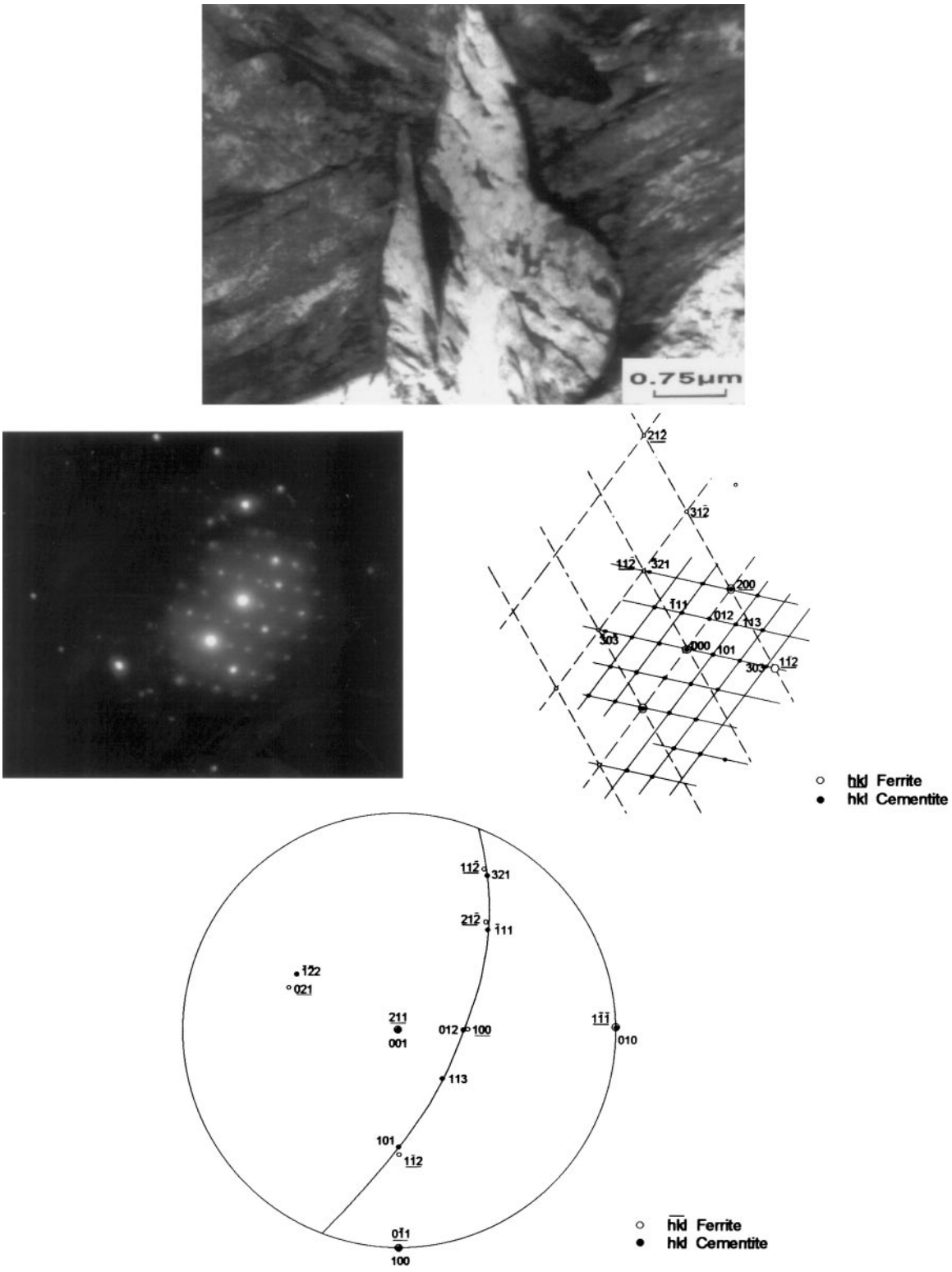

Fig. 6—Detail of the acicular ferrite microstructure obtained after 20 min of isothermal treatment at 400 °C. Diffraction pattern with spots corresponding to ferrite and cementite and stereographic projection showing the orientation relationship between both phases.

place at grain boundaries. This is not possible on particles, once the surface of the particle has been covered with ferrite. This explains the formation of individual plates. As the transformation temperature decreases, the branching tendency of the lower bainite leads to the formation of sheaves from the primary ferrite plate, without the need for repeated nucleation of units. This can explain the observed transition from a plate to sheaf morphology, as the transformation temperature decreases.

Probably the carbon-enrichment profile, which is expected to build up in austenite close to the interface of the primary plates, could play the most important role in determining

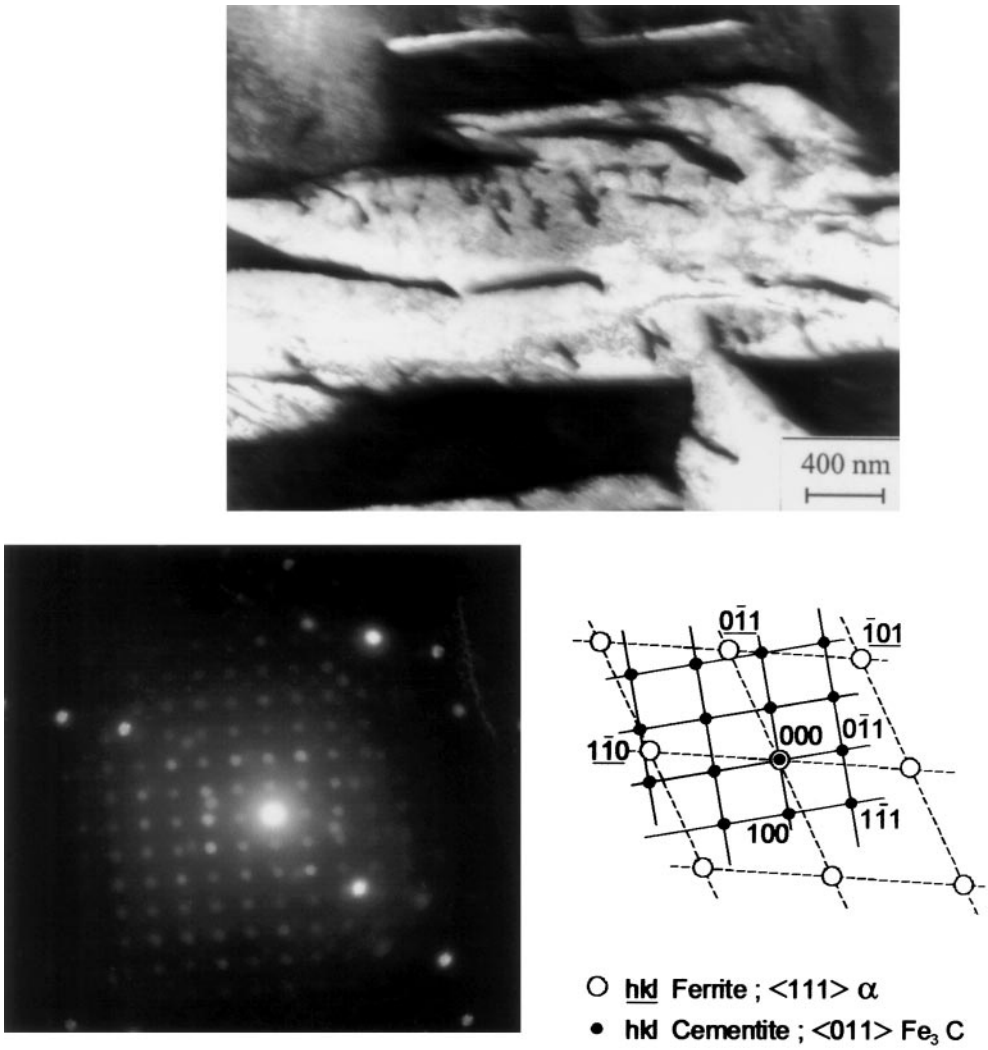

Fig. 7—Carbide precipitation in the microstructure obtained after 20 min of isothermal treatment at 400 °C. Diffraction pattern with spots corresponding to ferrite and cementite.

how the next units will form in acicular ferrite. For high temperatures, carbon would be able to diffuse away from the interface in short times, and new units would have the opportunity to nucleate on the primary plate faces, producing new ferrite variants. As the transformation temperature decreases, the carbon profile would become sharper in the austenite close to the interface. As a consequence, the stability of this phase would increase locally, and nucleation on the faces of the primary plates would be inhibited. However, the carbon-concentration profile in the austenite close to the tips of the primary plates is expected to be lower than at the faces. This would lead to the progress of the transformation, with the formation of new subunits presenting the same orientation relationship as the previous one. There may be two reasons for the formation of parallel units at low temperatures: the lower stability of the austenite close to the tip of the ferrite plate; and the strain field produced by the invariant plane-strain shape transformation, which favors the formation of the same variant as that of the primary plate at these sites.

Further growth of these subunits seems to be possible parallel to the primary plate, leaving a thin layer of carbon-enriched austenite (Figure 3(b)) between the different subunits. Afterward, these regions of austenite lead to the precipitation of cementite between the ferrite platelets.

V. CONCLUSIONS

1. In the present steel, acicular ferrite microstructures have been produced by isothermal treatments and exhibit two different morphologies: individual plates and sheaf formation in the upper- and lower-temperature range.
2. Plates are associated with upper acicular ferrite and sheaves correspond to lower acicular ferrite. In this last case, cementite precipitates are present at the ferrite unit interiors and between the different platelets.
3. The autocatalytic formation of new plates is expected to depend strongly on the carbon profile of the parent austenite in front of the interface with the primary plates. This profile would become sharper as the transformation temperature decreases and the diffusion in austenite, of the

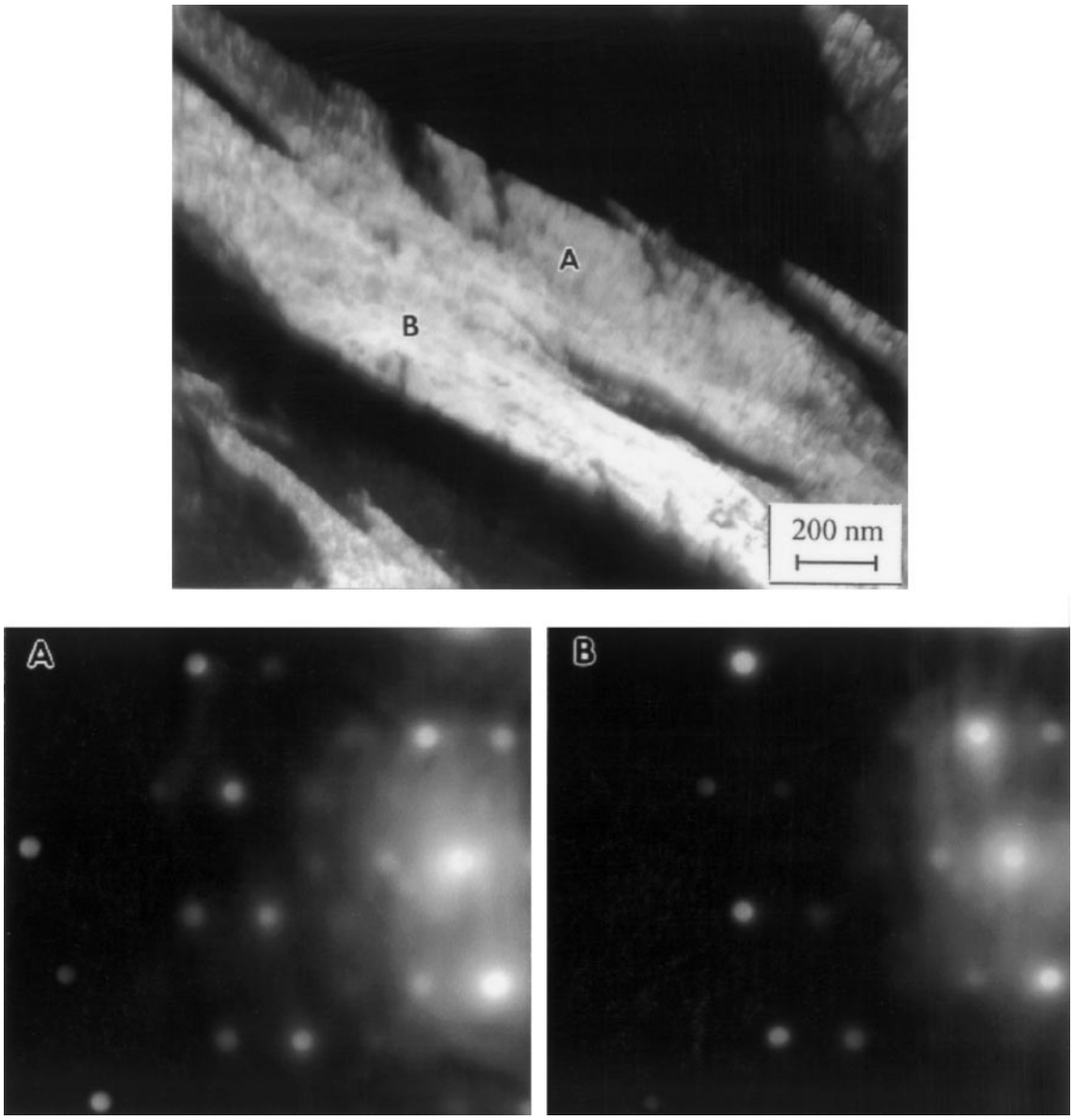

Fig. 8—TEM image of an intragranularly nucleated sheaf of two parallel ferrite plates. Diffraction patterns of both platelets showing the same cryst allographic orientation for them.

carbon rejected from the ferrite, becomes slower. Close to the ferrite tips, the carbon enrichment of the austenite could be low enough to allow the transformation to progress, leading to the formation of sheaves. At high temperatures, the diffusion of carbon is higher and plate formation on faces is possible.

ACKNOWLEDGMENTS

GSB Grupo Siderúrgico Vasco S.A. is thanked for providing the steel used in the present work and the CICYT for the financial support. IM acknowledges a "Formación de Investigadores" grant from the Departamento de Educación y Universidades of the Gobierno Vasco. B. Aizpurua is acknowledged for her assistance with the SEM work.

REFERENCES

1. H.K.D.H. Bhadeshia: *Bainite in Steels. Transformations, Microstructure and Properties*, 2nd Edition, The Institute of Materials, London, 2001, ch. 10.
2. Z. Zhang and R.A. Farrar: *Mater. Sci. Technol.*, 1996, vol. 12, pp. 237-60.
3. S.S. Babu and H.K.D.K. Bhadeshia: *Mater. Sci. Eng. A*, 1992, vol. 156, pp. 1-9.
4. M. Strangwood and H.K.D.H. Bhadeshia: *Proc. Int. Conf. Advances in Welding Science and Technology*, ASM, Cleveland, OH, 1987, pp. 187-91.
5. D.J. Abson and R.E. Dolby: *Weld. Inst. Res. Bull.*, 1987, vol. 19, pp. 202-07.
6. R.C. Cochrane and P.R. Kirkwood: in *Trends in Steels and Consumables for Welding*, The Welding Institute, Abingdon, 1978, pp. 103-21.
7. O. Grong and D.K. Matlock: *Int. Met. Rev.*, 1986, vol. 31 (1), pp. 27-48.
8. R.A. Ricks, P.R. Howell, and G.S. Barritte, Jr.: *Mater. Sci.*, 1982, vol. 17, pp. 732-40.
9. S. Ohkita, H. Homma, S. Tsushima, and N. Mori: *Aus. Welding J.*, 1984, pp. 29-36.

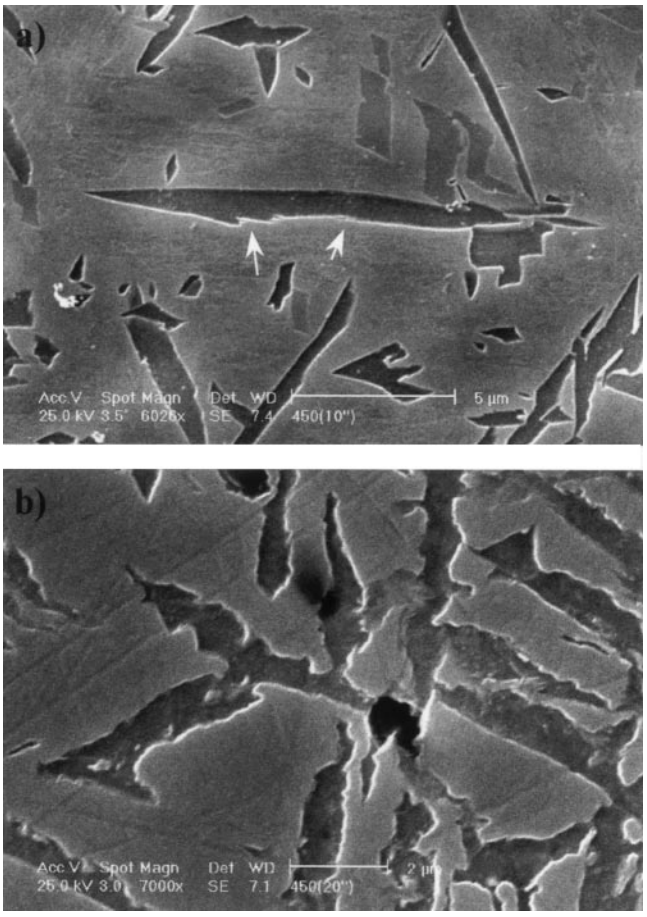

Fig. 9—Plate morphology produced at 450 °C after (*a*) 10 s and (*b*) 20 s of treatment.

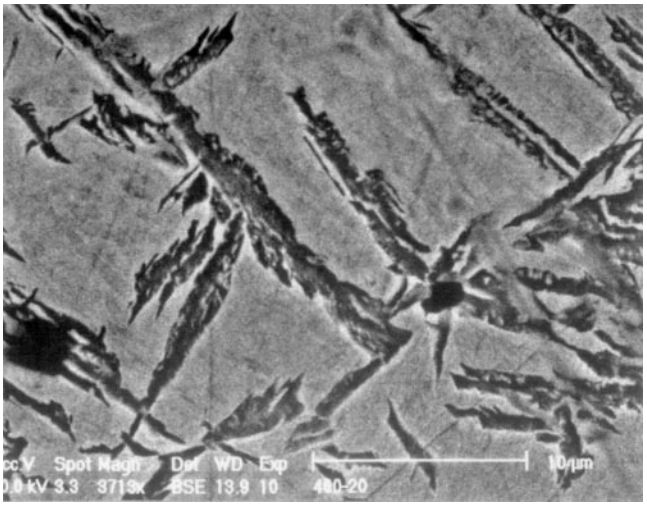

Fig. 10—Detail of the acicular ferrite microstructure produced after 20 s of treatment at 400 °C.

10. D.J. Abson, R.E. Dolby, and P.H.M. Hart: *Trends in Steels and Consumables for Welding*, Conf. Proc., The Welding Institute, Abingdon, 1987, pp. 75-101.
11. J.G. Garland and P.R. Kirkwood: *Met. Constr.*, 1975, vol. 7 (5), pp. 275-83.

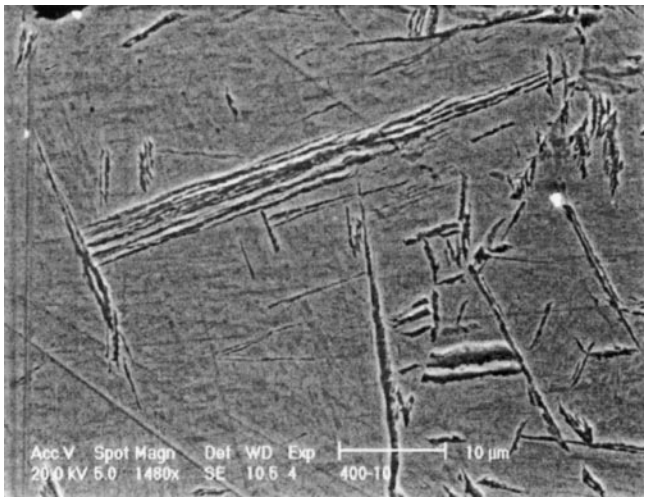

Fig. 11—Sheaf formation due to edge to face nucleation at the ferrite/austenite interface after 10 s of treatment at 400 °C (SEM image).

12. J.G. Garland and P.R. Kirkwood: *Met. Constr.*, 1975, vol. 7 (6), pp. 320-30.
13. J.M. Dowling, J.M. Corbett, and H.W. Kerr: *Metall. Trans. A*, 1986, vol. 17, pp. 1611-23.
14. O. Grong and D.K. Matlock: *Int. Met. Rev.*, 1986, vol. 31 (1), pp. 27-44.
15. E.S. Kayali, J.M. Corbett, and H.W. Kerr: *J. Mater. Sci. Lett.*, 1983, vol. 2, pp. 123-28.
16. S.K. Liu and D.L. Olson: *Weld. Res. Suppl.*, 1986, vol. 65, pp. 139s-149s.
17. M. Imagumbai, R. Chijiiwa, N. Aikawa, M. Nagumo, H. Homma, M. Matsuda, and H. Mimura: *HSLA Steels: Metallurgy and Aplications*, J.M. Gray, T. Ko, Z. Shouhua, W. Baorong, and X. Xishan, eds., ASM INTERNATIONAL, Metals Park, OH, 1985, pp. 557-66.
18. T. Ochi, T. Takahashi, and H. Takada: *Proc. 30th Mechanical Working and Steel Processing Conf.*, Iron and Steel Society, Warrendale, PA, 1989, vol. XXVI, pp. 65-72.
19. F.J. Barbaro, P. Krauklis, and K.E. Easterling: *Mater. Sci. Technol.*, 1989, vol. 5, pp. 1057-68.
20. F. Ishikawa, T. Takahashi, and T. Ochi: *Metall. Mater. Trans. A*, 1994, vol. 25A, pp. 929-36.
21. J.M. Gregg and H.K.D.H. Bhadeshia: *Acta Mater.*, 1997, vol. 45 (2), pp. 739-48.
22. K. Yamamoto, T. Hasegawa, and J. Takamura: *Iron Steel Inst. Jpn. Int.*, 1996, vol. 36, pp. 80-86.
23. E. Anelli, C. Andena, S. Matera, P. Harrison, I. Gutierrez, D. Porter, and T. Siwecki: ECSC Research Project Agreement 7210 PR/037 (97-D3.05a,b,c,d,e), 1998 Annual Report.
24. M.A. Linaza, J.L. Romero, J.M. Rodriguez-Ibabe, and J.J. Urcola: *Scripta Metall. Mater.*, 1993, vol. 29, pp. 1217-22.
25. M.A. Linaza, J.L. Romero, J.M. Rodriguez-Ibabe, and J.J. Urcola: *Scripta Metall. Mater.*, 1995, vol. 32, pp. 395-400.
26. I. Madariaga and I. Gutierrez: *Scripta Mater.*, 1997, vol. 37 (8), pp. 1185-92.
27. I. Madariaga, J.L. Romero, and I. Gutiérrez: *Metall. Mater. Trans. A*, 1998, vol. 29A, pp. 1003-15.
28. I. Madariaga and I. Gutiérrez: *Acta Mater.*, 1999, vol. 47 (3), pp. 951-60.
29. M. Díaz-Fuentes, I. Madariaga, J.M. Rodríguez-Ibabe, and I. Gutiérrez: *J. Construct. Steel Res.*, 1998, vol. 46 (1–3), pp. 413-14.
30. M. Díaz-Fuentes, I. Madariaga, and I. Gutiérrez: in *Microalloying in Steels*, J.M. Rodriguez-Ibabe, I. Gutierrez, and B. Lopez, eds., Materials Science Forum Vols. 284–286, Trans Tech Publications Ltd., Aedermannsdorf, Switzerland, 1998, pp. 245-52.
31. J.L. Romero, M.A. Linaza, J.I. San Martin, J.M. Rodriguez-Ibabe, and J.J. Urcola: *Rev. Met. CENIM*, 1996, vol. 32, pp. 1-13.
32. I. Madariaga and I. Gutiérrez: in *Microalloying in Steels*, J.M. Rodriguez-Ibabe, I. Gutierrez, and B. Lopez, eds., Materials Science Forum Vols. 284–286, Trans Tech Publications Ltd., Aedermannsdorf, Switzerland, 1998, pp. 419-26.

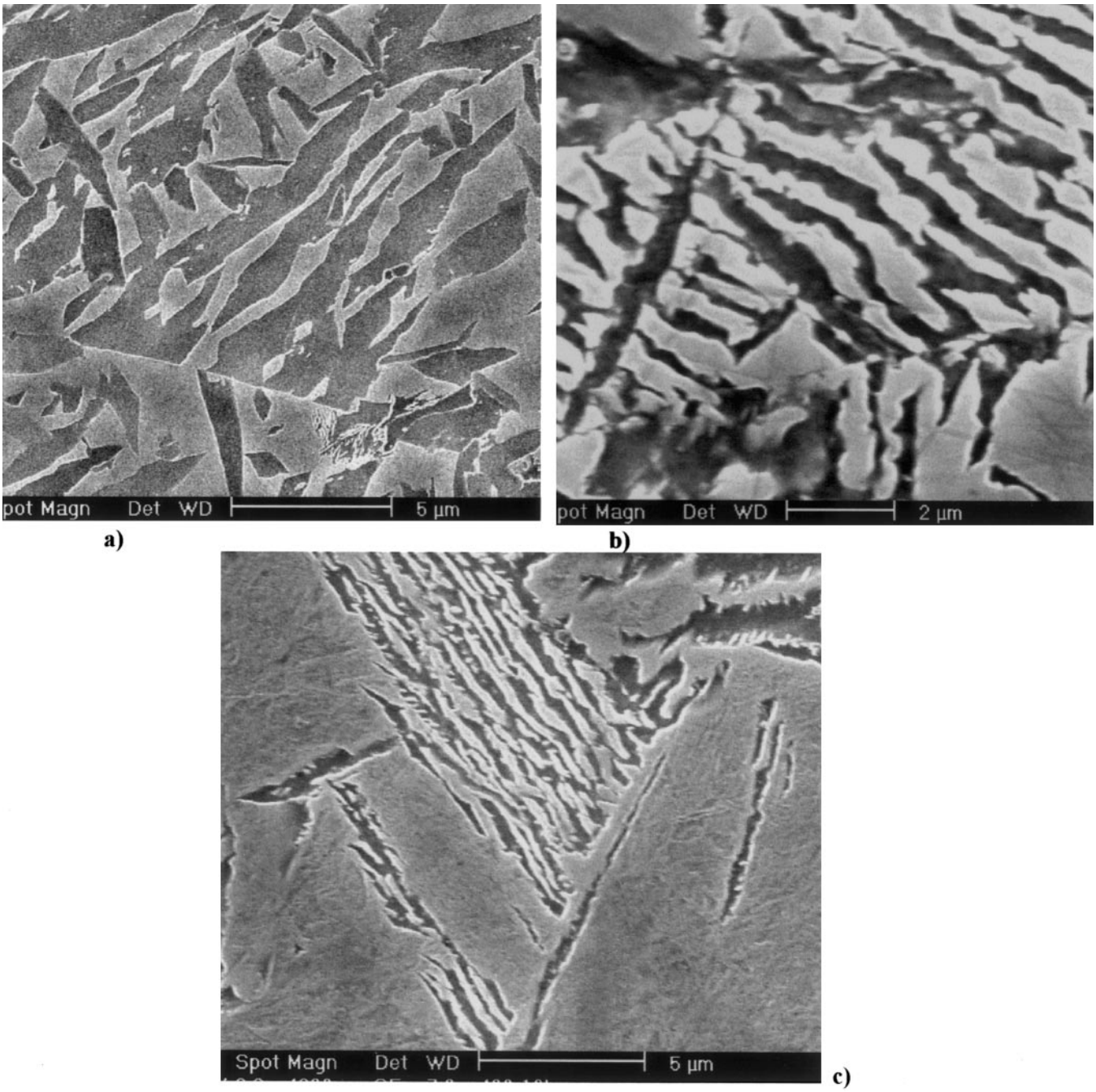

Fig. 12—Bainite areas formed in the steel samples treated (*a*) 10 s at 450 °C, (*b*) 30 s at 450 °C, and (*c*) 10 s at 400 °C.

33. I. Madariaga and I. Gutiérrez: *Conf. Proc. "TRATERMAT 98,"* Madrid, 1998, pp. 143-50.
34. B.D. Cullity: *Elements of X-ray Diffraction*, Addison-Wesley, Reading, MA, 1978, pp. 350-68.
35. C.H. Macgillavry and G.D. Rieck: *International Tables for X-Ray Crystallography*, The Kynoch Press, Birmingham, England, 1968, vol. 3.
36. G. Maeder, Y. Ramon, G. Tharel, and J. Barralis: *Mem. Sci. Rev. Met.*, 1975, pp. 397-405.
37. G.B. Olson and W.S. Owen: *New Aspects of Martensitic Transformation*, Institute of Metals, Tokyo, Japan, 1976, pp. 105-10.
38. J.R. Yang and H.K.D.H. Bhadeshia: in *Advances in Welding Science and Technology*, S.A. David, ed., ASM, Metals Park, OH, 1986, pp. 187-91.
39. S.J. Matas and R.F. Hehemann: *Trans. TMS-AIME*, 1961, vol. 221, pp. 179-85.
40. H.K.D.H. Bhadeshia and J.W. Christian: *Metall. Trans. A*, 1990, vol. 21A, pp. 767-97.
41. H.K.D.H. Bhadeshia: *Bainite in Steels. Transformations, Microstructure and Properties*, The Institute of Materials, London, 1992, ch. 3.
42. A. Bagaryatskii: *Dokl. Akad. Nauk SSSR*, 1950, vol. 73, p. 1161.
43. W. Pitsch: *Arch. Eisenhuettenwes.*, 1963, vol. 34, p. 381.
44. G.V. Kurdjumov and G. Sachs: *Z. Phys.*, 1930, vol. 64, p. 325.
45. H.K.D.H. Bhadeshia: *Worked Examples in the Geometry of Crystals*, The Institute of Metals, London, 1987.